**Ternary carbodiimide compound $Ba_{0.9}Sr_{0.1}NCN$ with distorted rutile-type structure**

Yuji Masubuhchi[1]*, Suzuka Miyazaki[2], Kotaro Fujii[3], Masatomo Yashima[3], Akira Miura[1], Mikiio Higuchi[1]

Affiliations:

[1]Faculty of Engineering, Hokkaido University, N13 W8, Kita-ku, Sapporo 060-8628, Hokkaido, Japan

[2]Graduate School of Chemical Sciences and Engineering, Hokkaido University, N13 W8, Kita-ku, Sapporo, 060-8628, Hokkaido, Japan

[3]Department of Chemistry, School of Science, Tokyo Institute of Technology, 2-12-1-W4-17, O-okayama, Meguro-ku, 152-8551, Tokyo, Japan

*Corresponding Author: Yuji Masubuchi; Faculty of Engineering, Hokkaido University, N13W8, Kita-ku, Sapporo 060-8628, Japan; Tel: +81-(0)11-706-6742; E-mail: yuji-mas@eng.hokudai.ac.jp

**Abstract**

Ternary carbodiimides, $Ba_{1-x}Sr_xNCN$ ($x$ = 0, 0.1, 0.2, 0.5, 0.8, and 1.0) were prepared by an ammonolysis reaction with a $(Ba,Sr)CO_3$ precursor obtained by a polymerized complex method. A new orthorhombic carbodiimide was obtained at $x$ = 0.1. It coexists with SrNCN-type solid solutions between $x$ = 0.2 and 0.5. The crystal structure of $Ba_{0.9}Sr_{0.1}NCN$ was determined using single-crystal X-ray and powder neutron diffraction data, and was found to adopt an orthorhombic *Pnnm* crystal structure. In this structure, both $Ba^{2+}$ and $Sr^{2+}$ cations are situated in an octahedron of N atoms of $NCN^{2-}$ anionic groups, and the $(Ba/Sr)N_6$ octahedra form a distorted rutile-type structure with C atoms bridging the N atoms.

**Keywords**

Carbodiimide; crystal structure; distorted rutile-type structure;

## Introduction

Metal carbodiimides and cyanamides are interesting solid-state inorganic materials that exhibit a nitrogen-related pseudo-oxide chemistry, because $N=C=N^{2-}$ carbodiimide and $N-C\equiv N^{2-}$ cyanamide anionic groups can replace $O^{2-}$ anions. Many binary carbodiimides have been prepared for alkali [1-3], alkaline earth [4,5], main-group metal [6], transition metals [7-10], and rare-earth metal phases [11,12]. More recently, ternary and higher order compounds such as $AEZn(NCN)_2$ ($AE$ = $Sr^{2+}$ and $Ba^{2+}$) and $LiSr_2M(NCN)_4$, ($M$ = $Al^{3+}$ and $Ga^{3+}$) have also been synthesized [13-16]. A limited number of binary cyanamides have also been reported for HgNCN, PbNCN, AgNCN, and CdNCN [17-20].

Many of the carbodiimides and cyanamides, especially thermally unstable compounds, have been synthesized by solid state metathesis reactions between metal halides and carbodiimides. $Li_2NCN$ and ZnNCN have been used as $NCN^{2-}$ anion sources and form LiCl and $ZnCl_2$ by-products, respectively, after a low-temperature reaction with metal chlorides at approximately 773 K [9,12]. High-temperature nitridation reactions of metal carbonates under an ammonia flow have also been applied to synthesize the respective carbodiimides [21,22]. Rhombohedral BaNCN was synthesized by the reaction of $Ba_3N_2$ and melamine under an Ar flow, while a tetragonal polymorph was recently obtained by the ammonolysis of $BaCO_3$ [4,23,24].

Transition metal carbodiimides *TM*NCN (*TM* = Mn, Fe, Co, Cu, Zn, Ni), have been studied for their electrochemical activities in Li and Na ion batteries with high reversible capacities [25-27]. Photochemical activities of cobalt and copper carbodiimides have also been reported, and the former exhibited high photocatalytic water oxidation activity under irradiation by visible light [28,29]. Alkaline earth metal and rare-earth metal carbodiimides have also been applied as host materials for doping of photoluminescence centers such as $Eu^{2+}$, $Eu^{3+}$, $Ce^{3+}$, and $Mn^{2+}$ [22,23,30-33]. A divalent Eu-doped tetragonal BaNCN red phosphor exhibits a large shift in the luminescence wavelength depending on both temperature and applied pressure, since the tetragonal phase has a flexible framework and the crystal field splitting of the 5*d* energy levels of the $Eu^{2+}$ ions varies depending on the bond length [23,34]. Anomalous thermal and mechanical properties have also been reported for beta-$Si(NCN)_2$ and *TM*$(NCN)_2$ (*TM* = Zr and Hf) which show negative thermal expansion and near-zero thermal expansion, respectively [35,36].

In the field of metal oxide chemistry, partial substitution of a metal cation with another having different ionic size is commonplace to prepare solid solutions or intermediate compounds between the end members. In these compounds, two or more metal cations occupying an identical position can have varying numbers of neighboring anions, bond lengths and bond angles from their counterparts in the end members, because of the intermediate size of the

crystallographic site, thus forming a novel crystal structure. This study focusses on the preparation of ternary carbodiimides between BaNCN and SrNCN *via* an ammonolysis reaction of the respective carbonate precursors. The crystal structure of the novel Ba/Sr carbodiimide was analyzed using both single crystal XRD and powder neutron diffraction. This carbodiimide crystallized in an orthorhombic lattice, with a statistical distribution of $Ba^{2+}$ and $Sr^{2+}$ forming a rutile-like $(Ba/Sr)N_6$ polyhedral network bridged by $NCN^{2-}$ anions.

## Experimental

### Synthesis

$Ba_{1-x}Sr_xNCN$ ($x$ = 0, 0.1, 0.2, 0.4, 0.5, 0.8, and 1.0) were obtained by nitridation of $(Ba_{1-x}Sr_x)CO_3$ precursors prepared by a polymerized complex method starting from $BaCO_3$ (99.9 % purity, FUJIFILM Wako Pure Chemical Co.), $SrCO_3$ (99.9% purity, FUJIFILM Wako Pure Chemical Co.), citric acid (>98.0 % purity, FUJIFILM Wako Pure Chemical Co.) and propylene glycol (>98.0 %, FUJIFILM Wako Pure Chemical Co.) [37,38]. The carbonate precursors were nitrided under 100 mL/min $NH_3$ flow at 1173 K for 15 h. The nitrided products were air-sensitive, so the characterization described below was performed under either a dry $N_2$ or Ar atmosphere.

### Characterization

Crystalline phases were characterized using powder X-ray diffraction (XRD: Rigaku, Ultima IV) with Cu-*Kα* radiation. The products were contained in an air tight sample holder filled with dry Ar. The crystal structure of $Ba_{1-x}Sr_xNCN$ at $x$ = 0.1 was investigated by the single-crystal XRD technique using a Rigaku XtaLAB Pro diffractometer (Mo-*Kα* radiation). The single crystal was protected by oil from atmospheric moisture and measurement was performed at 123 K to avoid a degradation. Atomic positions were determined by the charge flipping method using SuperFlip [39] followed by structure refinements using SHELXL-2018 [40]. The crystal structures were drawn using the VESTA program [41]. Neutron diffraction (ND) data were collected at the BL09 (SPICA) beamline of the Japan Proton Accelerator Research Complex (J-PARC) at 298 K and analyzed with the software Z-Rietveld (Windows ver. 1.1.1.0914) [42]. The temperature dependence of the lattice parameters was also investigated using synchrotron powder XRD (SXRD) data of $Ba_{0.9}Sr_{0.1}NCN$ powder at the BL02B2 beam-line of SPring-8 over the temperature range from 90 K to 300 K. The wavelength of the incident X-ray used for the refinements was 0.0496353 nm. The X-ray diffraction data were analyzed by the Rietveld method using RIETAN-FP [43].

The Ba and Sr contents in the product prepared at $x$ = 0.1 were determined by inductively coupled plasma-atomic emission spectroscopy (ICP-AES: Shimadzu, ICPE-9000) after dissolving a 10 mg sample in dilute nitric acid. The C, H, and N contents were assessed via

C/H/N analysis (Exeter Analytical, Inc., CE440). Fourier transform infrared spectroscopy (FT-IR) was performed with an FT-IR/4700 spectrometer (Jasco). The test specimens were prepared by sandwiching the powder product between KBr plates and pressing the sample into a pellet under a dry Ar atmosphere.

**Result and discussion**

A nitridation reaction under flowing $NH_3$ was performed with the carbonate precursors $Ba_{1-x}Sr_xCO_3$. The powder XRD patterns of the nitrided products are shown in Fig. 1. The pattern of tetragonal BaNCN and orthorhombic SrNCN are observed for the products at $x$ = 0 and 1.0, respectively. The tetragonal BaNCN was contaminated with a small amount of new orthorhombic phase as mentioned later. The diffraction angles of the orthorhombic SrNCN shifted toward lower angle on incorporation of Ba at $x$ = 0.8, implying the formation of an orthorhombic type carbodiimide solid solution. A new orthorhombic crystalline phase which cannot be indexed by the above mentioned tetragonal and orthorhombic phases appears at $x$ = 0.1. It coexists with the orthorhombic solid solutions from $x$ = 0.2 to 0.5. The chemical composition of the nitrided product at $x$ = 0.1 was analyzed by combination of ICP-AES and C/H/N analysis. The Ba and Sr concentrations in the product were found to be 69.8(8) and 4.9(1) wt%, respectively, while the C, H, and N contents were 6.9(3), <0.3, and 15.8(3) wt%,

respectively. The H content was below the detection limit of the C/H/N analysis. From these data, the chemical formula of the compound at $x$ = 0.1 was determined to be $Ba_{0.90(1)}Sr_{0.099(1)}C_{1.01(4)}N_{1.99(4)}$, which agrees well with the nominal composition $Ba_{0.9}Sr_{0.1}NCN$.

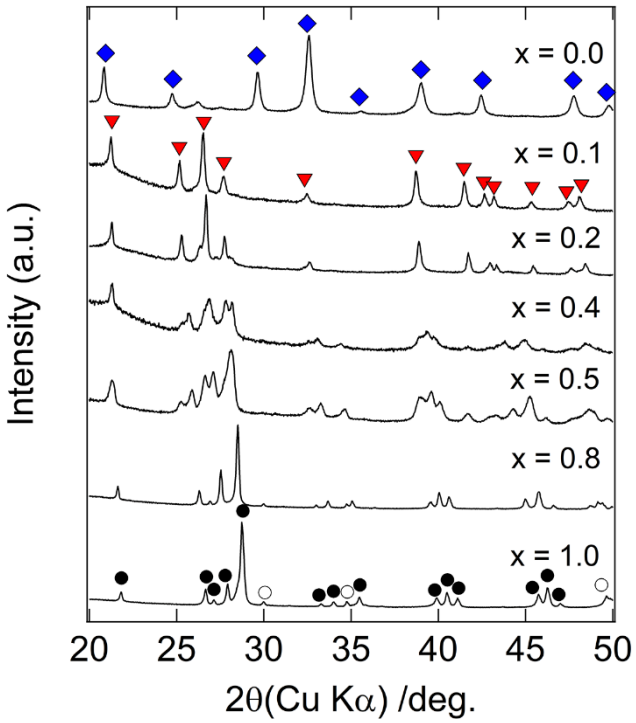


Figure 1 XRD patterns of nitrided products obtained from $(Ba_{1-x}Sr_x)CO_3$ precursors with $x$ = 0~1. Diffraction lines marked with blue diamonds, red triangles, filled circles and open circles indicate tetragonal BaNCN, the novel crystalline phase, orthorhombic SrNCN and SrO, respectively.

The crystal structure of $Ba_{0.9}Sr_{0.1}NCN$ was analyzed by single-crystal XRD at 123 K. The structure was refined in the orthorhombic space group *Pnnm* (no. 58) with $a$ = 0.55224(7)

nm, *b* = 0.64455(8) nm and *c* = 0.42411(6) nm, and *Z* = 2, as summarized in Table 1. Atomic coordinates are given in Table 2. Anisotropic displacement parameters (ADPs) were only adopted for Ba/Sr and N atoms. The ADPs of C atoms was analyzed to be negative values, maybe due to the poor quality of the diffraction data resulting from small crystal size and/or instability of the carbodiimide during the measurement. Therefore, isotropic displacement parameter for the C atom was only analyzed and the value is listed in Table 2. $Ba^{2+}$ and $Sr^{2+}$ cations are situated at the 2*a* site. The Ba/Sr and $NCN^{2-}$ are three-dimensionally arranged in this structure similar to the configuration in tetragonal and rhombohedral BaNCN, while SrNCN and CaNCN adopt a layer structure of alkaline earth metal cations and $NCN^{2-}$ anions. A view of the structure is depicted in Fig. 2. The $NCN^{2-}$ anions are parallel to the *a*-*b* plane and directed alternately toward <1-10> and <110> as shown in Fig. 2(c). Ba/Sr cations are coordinated with six N atoms belonging to the $NCN^{2-}$ anions to form a $(Ba/Sr)N_6$ octahedron as shown in Fig. 3(a). The octahedra are connected via edge-sharing along the *c*-axis and corner-sharing in the *a*-*b* plane. The $NCN^{2-}$ anion is in an octahedral site surrounded by Ba/Sr cations (Fig. 3(b)). The ordered arrangement of the $NCN^{2-}$ anions was also confirmed by structure refinement based on the powder ND data collected at 298 K. The ND profile and refined structural parameters are shown in Fig. S1 and Table S1 in the electronic supplementary information (ESI) respectively. The experimental diffraction profile is in good

agreement with the calculated pattern, although a minor quantity of tetragonal BaNCN coexists with the orthorhombic phase. By virtue of the scattering contrast between the elements attained in neutron experiments, we were able to confirm the ordering of the $NCN^{2-}$ orientation. Nitrogen site splitting model similar to the $La_2O_2NCN$ [44], which is difficult to be distinguished from the ordered arrangement by using XRD, was successfully excluded by the refinement using ND data. The C-N bond length estimated using the ND data observed at room temperature is 0.12230(3) nm, which is close to values reported for C-N double bonds in metal carbodiimides [4]. The FT-IR spectrum of this product exhibits an asymmetric stretch peak ($\nu_{as}$) at 1950 $cm^{-1}$ and deformation peaks (δ) at 655 and 675 $cm^{-1}$ (see Fig. S2). These peak positions are in good agreement with those reported for both rhombohedral and tetragonal BaNCN, which are metal carbodiimides having symmetric N=C=N double bonds [4,22]. The Ba/Sr-N bond lengths in the orthorhombic carbodiimide are 0.280175(11) and 0.27983(2) nm, which are shorter than the values reported for tetragonal BaNCN with square antiprism coordinated $Ba^{2+}$ cations (0.2928 nm) and longer than the Sr-N bond lengths in orthorhombic SrNCN (ca. 0.2628 nm) with octahedral coordination around $Sr^{2+}$. The shorter bond lengths and smaller coordination number around the Ba/Sr site than those of tetragonal BaNCN are attributed to the substitution of the smaller $Sr^{2+}$ ion for $Ba^{2+}$ on the site. $Ba/Sr^{2+}$ cations and $NCN^{2-}$ anions form a distorted rock-salt like arrangement in the orthorhombic

$Ba_{0.9}Sr_{0.1}NCN$. Orthorhombic SrNCN has also a rock-salt like distribution, in which octahedra around $Sr^{2+}$ cations are more distorted than that in the orthorhombic $Ba_{0.9}Sr_{0.1}NCN$. On the other hand, CsCl like configuration of $Ba^{2+}$ and $NCN^{2-}$ is found in the tetragonal BaNCN. The $NCN^{2-}$ anions in the $Ba_{0.9}Sr_{0.1}NCN$ and tetragonal BaNCN are parallel to the ab-plane and stacked with Ba/Sr and Ba cation along the c-axis, respectively. $Ba_{0.9}Sr_{0.1}NCN$ represents the first example of a ternary carbodiimide consisting of two kinds of alkaline earth metals. In the structure, both $Ba^{2+}$ and $Sr^{2+}$ cations occupy the same crystallographic site, with bond lengths and local coordination around the cation site intermediate between those of the end members, similar to ternary oxide chemistry.

Table 1 Crystal data and refinement result at 123 K for $Ba_{0.9}Sr_{0.1}NCN$ obtained by ammonolysis reaction of $Ba_{0.9}Sr_{0.1}CO_3$ precursor.

| | |
|---|---|
| Chemical formula | $Ba_{0.9}Sr_{0.1}NCN$ |
| Formula weight, $M_r$ (g mol$^{-1}$) | 172.40 |
| Crystal form, color | platelet, colorless |
| Crystal size, mm$^3$ | 0.015×0.010×0.005 |
| Radiation wavelength, $\lambda$ (nm) | 0.71073 |
| Temperature, $T$ (K) | 123 |
| Crystal system | Orthorhombic |
| Space group | *Pnnm* (No. 58) |
| Unit cell dimensions, $a$ (nm) | 0.55224(7) |
| $b$ (nm) | 0.64455(8) |
| $c$ (nm) | 0.42411(6) |
| Unit cell volume, $V$ (nm$^3$) | 0.15096(3) |
| $Z$ | 2 |
| Calculated density, $D_{cal}$ (Mg m$^{-3}$) | 3.793 |
| Absorption coefficient, $\mu$ (mm$^{-1}$) | 13.322 |
| Absorption correction | Multi-scan |
| Limiting Indices | $-6 \le h \le 6$ |
| | $-8 \le k \le 8$ |
| | $-5 \le l \le 5$ |
| Number of reflections | 203 |
| Weight parameters, $a$, $b$ | 0.1035, 1.369 |
| Goodness-of-fit on $F^2$, $S$ | 1.208 |
| $R_1$, $wR_2$ ($I > 2\sigma(I)$) | 0.0612, 0.1539 |
| $R_1$, $wR_2$ (all data) | 0.0930, 0.1646 |

$R_1 = \Sigma||F_o| - |F_c||/\Sigma|F_o|$. $wR_2 = [\Sigma w(F_o^2 - F_c^2)^2/\Sigma(wF_o^2)^2]^{1/2}$, $w = 1/[\sigma^2(F_o^2) + (aP)^2 + bP]$, where $F_o$ is the observed structure factor, $F_c$ is the calculated structure factor, $\sigma$ is the standard derivation of $F_o^2$, and $P = (F_o^2 + 2F_c^2)/3$. $S = [\Sigma w(F_o^2 - F_c^2)^2/(n - p)]^{1/2}$, where n is the number of reflections and $p$ is the total number of parameters refined.

Table 2 Atomic coordinates for $Ba_{0.9}Sr_{0.1}NCN$ at 123 K.

| Atom | Site | Occ. | x | y | z | $U_{iso}$ (Å$^2$) |
|---|---|---|---|---|---|---|
| Ba/Sr | 2*a* | 0.9/0.1 | 0 | 0 | 0 | 0.0164(7) |
| C | 2*c* | 1 | 0.5 | 0 | 0.5 | 0.011(5) |
| N | 4*g* | 1 | 0.193(4) | 0.397(3) | 0 | 0.017(4) |

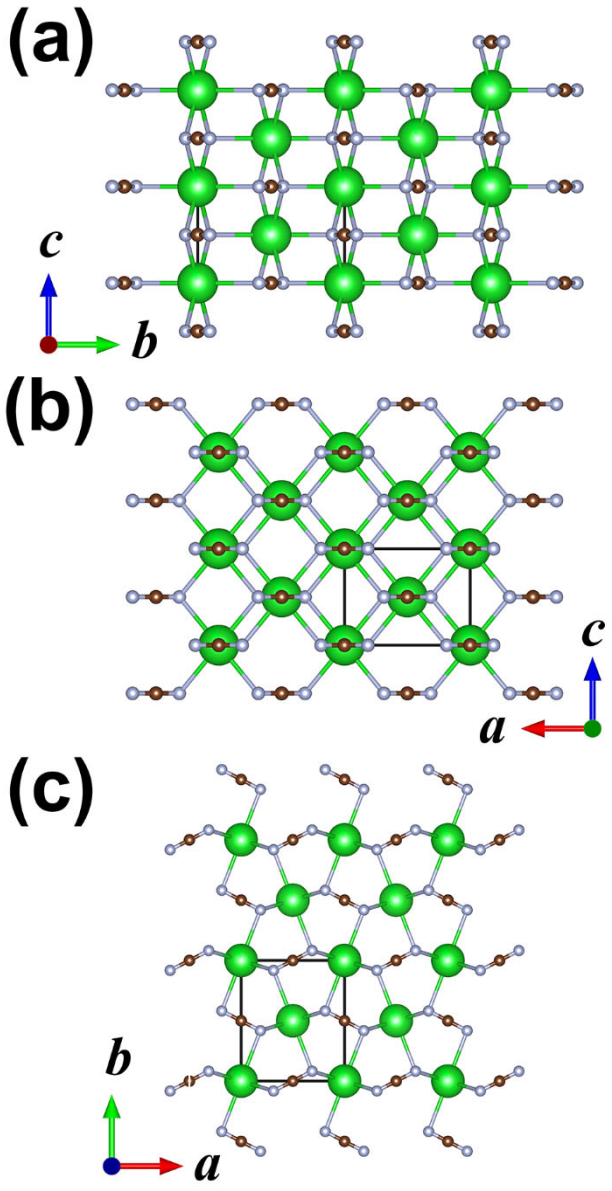


Figure 2 Images of the crystal structure orthorhombic $Ba_{0.9}Sr_{0.1}NCN$ along (a) *a*-, (b) *b*-, and (c) *c*-axis. Green, brown, and grey spheres correspond to Ba/Sr, C and N, respectively.

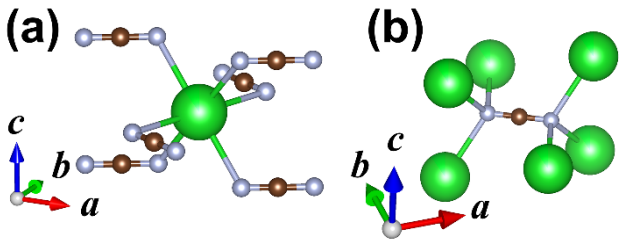


Figure 3 Coordination around (a) ($Ba_{0.9}Sr_{0.1}$) site and (b) $NCN^{2-}$ anion.

The nitrogen atoms form hexagonal packing along the *a*-axis. Half of the octahedral holes are occupied by Ba/Sr cations, forming (Ba/Sr)$N_6$ octahedra. The (Ba/Sr)$N_6$ octahedra have a network structure analogous to the rutile-type $TiO_2$ structure, as shown in Fig. 4. (Ba/Sr)$N_6$ octahedra connect *via* edge-sharing along the *c*-axis to form octahedral chains, which are linked by sharing the N vertices in the *a*-*b* plane similar to the arrangement in rutile-type $TiO_2$. Distortion from the rutile-type structure situating the cation site in Wyckoff position in 2*a* and nitrogen in position 4*g,* indicates that the crystal structure of $Ba_{0.9}Sr_{0.1}NCN$ is categorized into a distorted rutile-type structure $CaCl_2$ as following the definition by Baur [45]. The coordination octahedra (Ba/Sr)$N_6$ are considerably more rotated rather than in $CaCl_2$. Carbon atoms occupy the vacant octahedral holes of hexagonal N packing and bridge the two N atoms, forming a $N=C=N^{2-}$ anion. The $N=C=N^{2-}$ anions tilt the (Ba/Sr)$N_6$ octahedral chains around the *c*-axis (Fig. 4). Additional bond bridging two octahedra in the rutile-type derivatives

appears in marcatise, $FeS_2$, in which the S-S bond distorts the octahedral chains as shown in Fig. 4(d). Each N atoms in $Ba_{0.9}Sr_{0.1}NCN$ is bonded to three Ba/Sr atoms and one C atom, similar to a coordination around S atoms in $FeS_2$. This similarity suggests that the orthorhombic $Ba_{0.9}Sr_{0.1}NCN$ is one of the marcasite derivatives, which has close relation with distorted rutile-type structure. Hydrogen bond between OH groups and oxygen has also been reported in anion ordered rutile-type metal oxyhydroxides resulting in an octahedral distortion [45,46].

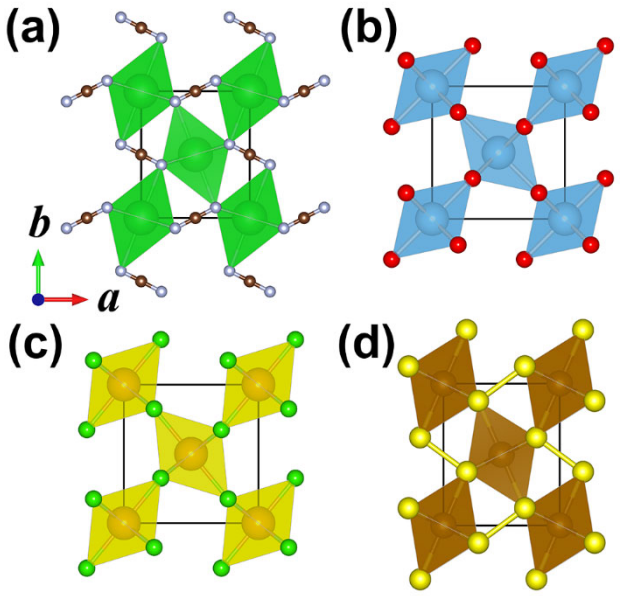


Figure 4 Octahedral networks viewed along *c*-axis for (a) orthorhombic $Ba_{0.9}Sr_{0.1}NCN$, (b) tetragonal rutile-type $TiO_2$, (c) distorted rutile-type $CaCl_2$, and (d) marcasite, $FeS_2$.

The temperature dependence of the lattice parameters of $Ba_{0.9}Sr_{0.1}NCN$ was examined between 90 K and 300 K based on the SXRD data. No phase transition for the orthorhombic

phase was observed in the SXRD data. The normalized lattice parameters are plotted in Fig. 5. The lattice shrinkage along the *c*-axis was estimated to be 0.2% over the temperature range, which was two and four times larger than those along the *a*-axis and *b*-axis, respectively. The linear thermal expansion coefficients (TECs) of the orthorhombic phase were estimated to be $\alpha_a = 9.0\times10^{-6}$ $K^{-1}$, $\alpha_b = 2.6\times10^{-6}$ $K^{-1}$, and $\alpha_c = 1.4\times10^{-5}$ $K^{-1}$ at 290K. Preferential shrinkage along the *c*-axis was also observed in tetragonal BaNCN [22]. The TECs of the tetragonal phase are $\alpha_a = 1.5\times10^{-5}$ $K^{-1}$ and $\alpha_c = 2.3\times10^{-5}$ $K^{-1}$ at 290K. Both structures exhibit stacking of Ba/Sr cations and $NCN^{2-}$ anions along the *c*-axis, and the large TEC is observed perpendicular to the $NCN^{2-}$ anion. Highly anisotropic thermal expansion was reported for $Hf(NCN)_2$ and SnNCN. In the former structure, negative thermal expansion along the *a*-axis and positive thermal expansion along the *b*- and *c*-axes were predicted based on DFT calculations [36,47]. Their anisotropic expansion can be related to the wine-rack-like open channel structure. In orthorhombic $Ba_{0.9}Sr_{0.1}NCN$, all of the octahedral sites in the hexagonal packing of N atoms are occupied by Ba/Sr and C alternatively. $NCN^{2-}$ anions aligned in the *a*-*b* plane might suppress the thermal expansion along the *a*- and *b*-axes.

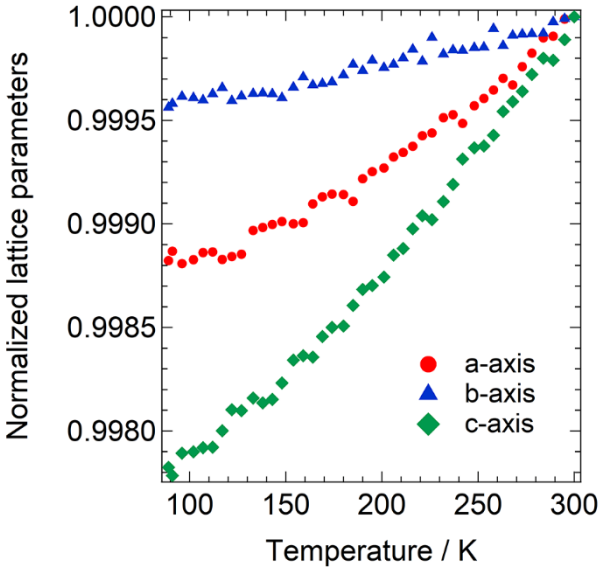


Figure 5 Temperature dependence of the normalized lattice parameters of orthorhombic $Ba_{0.9}Sr_{0.1}NCN$.

**Conclusion**

A new ternary carbodiimide with an orthorhombic structure, $Ba_{0.9}Sr_{0.1}NCN$, was prepared by nitridation of a $(Ba_{1-x}Sr_x)CO_3$ precursor at $x$ = 0.1 under an $NH_3$ flow. The crystal structure is analogous to that of distorted rutile-type derivative, in which $(Ba/Sr)N_6$ octahedra are edge-shared along the *c*-axis and corner shared in the *a*-*b* plane, and C atoms bridge two N atoms to form $N=C=N^{2-}$ anions. This is the first report of a ternary carbodiimide containing two alkaline earth metals on the same crystallographic site and demonstrates that the crystal structure can be varied *via* tuning of the cation size in a ternary carbodiimide, as in a ternary oxide. This work will open a new way for the preparation of novel carbodiimide compounds.

**Acknowledgements**

This work was partly supported by the JSPS Grants-in-Aid for Scientific Research on Innovative Areas “Mixed Anion” (grant numbers JP16H06438, JP16H06439, JP16H06440, JP19H04682). The neutron diffraction experiment at J-PARC was performed with the approval of Proposal no. 2017L1302. The synchrotron radiation experiment was performed at the BL02B2 beam-line of SPring-8 with the approval of the Japan Synchrotron Radiation Research Institute (JASRI) (Proposal No. 2018B1246).

**References**

[1] M. G. Down, M. J. Haley, P. Hubberstey, R. J. Pulham and A. E. Thunder, Synthesis of the dilithium salt of cyanamide in liquid lithium ; X-ray crystal structure of $Li_2NCN$, J. Chem. Soc. Chem. Commun. (1978) 52-53.

[2] K. M. Adams, M. J. Cooper and M. J. Sole, The structures of some inorganic cyanamides. I. Preparation of single crystals and preliminary studies, Acta Crystallogr. 17 (1964) 1449-1451.

[3] M. Becker and M. Jansen, Synthesis of potassium cyanamide, and crystal structure determination by pareto optimisation of the cost functions ‘lattice energy’ and ‘powder

intensities', Solid State Sci. 2 (2000) 711-715.

[4] U. Berger and W. Schnick, Synthesis, crystal structures, and vibrational spectroscopic properties of $MgCN_2$, $SrCN_2$, and $BaCN_2$, J. Alloys Compd. 206 (1994) 179-184.

[5] A. Cochet, Untersuchungen über die Azotierung des Calciumcarbides, Angew. Chem. 44 (1931) 367-372.

[6] R. Riedel, A. Greiner. G. Miehe, W. Dressler, H. Fuess, J. Bill, and F. Aldinger, The first crystalline solids in the ternary Si-C-N system, Angew. Chem. Int. Ed. Engl. 36 (1997) 603-606.

[7] X. Liu, M. Krott, P. Muller, C. Hu, H. Lueken, and R. Dronskowski, Synthesis, Crystal structure, and properties of MnNCN, the first carbodiimide of a magnetic transition metal, Inorg. Chem. 44 (2005) 3001-3003.

[8] X. Liu, L. Stork, M. Speldrich, H. Lueken, and R. Dronskowski, FeNCN and $Fe(NCNH)_2$: Synthesis, structure, and magnetic properties of a nitrogen-based pseudo-oxide and hydroxide of divalent Iron, Chem. Eur. J. 15 (2009) 1-1561.

[9] X. Tang, H. Xiang, X. Liu, M. Speldrich, and R. Dronskowski, A ferromagnetic carbodiimide: $Cr_2(NCN)_3$, Angew. Chem. Int. Ed. 49 (2010) 4738-4742.

[10] K. Dolabdjian, A. Kobald, C. P. Romao and H. J. Meyer, Synthesis and thermoelastic properties of $Zr(CN_2)_2$ and $Hf(CN_2)_2$, Dalton Trans. 47 (2018) 10249-10255.

[11] O. Reckeweg and F. J. DiSalvo, $EuCN_2$ - The first, but not quite unexpected ternary rare earth metal cyanamide, Z. Anorg. Allg. Chem. 629 (2003) 177-179.

[12] M. Neukirch, S. Tragl, and H. J. Meyer, Syntheses and structural properties of rare earth carbodiimides, Inorg. Chem. 45 (2006) 8188-8193.

[13] A. J. Corkett, P. M. Konze, and R. Dronskowski, The ternary post-transition metal carbodiimide $SrZn(NCN)_2$, Z. Anorg. Allg. Chem., 643 (2017) 1456-1461.

[14] A. J. Corkett, P. M. Konze and R. Dronskowski, Synthesis, crystal structure, and chemical-bonding analysis of $BaZn(NCN)_2$, Inorganics 6 (2018) 1-10.

[15] M. Kalmutzki, M. Strobele, S. Kroeker, J. E. C. Wren, and H. J. Meyer, Synthesis and characterization of the first tetracyanamidogallate, Eur. J. Inorg. Chem. 2013 (2013) 6091-6096.

[16] L. Unverfehrt, M. Kalmutzki, M. Strobele and H. J. Meyer, Solid state synthesis of homoleptic tetracyanamidoaluminates, Dalton Trans. 40 (2011) 9921-9924.

[17] X. Liu, P. Muller, P. Kroll, and R. Dronskowski, Synthesis, structure determination, and quantum-chemical characterization of an alternate HgNCN polymorph, Inorg. Chem. 41 (2002) 4259-4265.

[18] X. Liu, A. Decker, D. Schmitz, and R. Dronskowski, Crystal structure refinement of lead cyanamide and the stiffness of the cyanamide anion, Z. Anorg. Allg. Chem. 626 (2000) 103-

105.

[19] M. Becker, J. Nuss, and M. Jansen, Crystal structure and spectroscopic data of silver cyanamide, Z. Naturforsch. B 55 (2000) 383-385.

[20] G. Baldinozzi, B. Malinowska, M. Rakib, and G. Durand, Crystal structure and characterization of cadmium cyanamide, J. Mater. Chem. 12 (2002) 268-272.

[21] A. Perret and A. M. Krawezynski, Recherches sur les cyanamides metalliques, Helv. Chim. Acta 15 (1932) 1009-1022.

[22] S. Yuan, Y. Yang, F. Chevire, F. Tessier, X. Zhang, and G. Chen, Photoluminescence of $Eu^{2+}$-doped strontium cyanamide: a novel host lattice for $Eu^{2+}$, J. Am. Ceram. Soc. 93 (2010) 3052-3055.

[23] Y. Masubuchi, S. Nishitani, A. Hosono, Y. Kitagawa, J. Ueda, S. Tanabe, H. Yamane, M. Higuchi and S. Kikkawa, Red-emission over a wide range of wavelength at various temperatures from tetragonal $BaCN_2$:$Eu^{2+}$, J. Mater. Chem. C 6 (2018) 6370-6377.

[24] A. Hosono, R. P. Stoffel, Y. Masubuchi, R. Dronskowski, and S. Kikkawa, Melting behavior of alkaline-earth metal carbodiimides and their thermochemistry from first-principles, Inorg. Chem. 58 (2019) 8938-8942.

[25] M. T. Sougrati, A. Darwiche, X. Liu, A. Mahmoud, R. P. Hermann, S. Jouen, L. Monconduit, R. Dronskowski, and L. Stievano, Transition-metal carbodiimides as molecular

negative electrode materials for lithium- and sodium-ion batteries with excellent cycling properties, Angew. Chem. Int. Ed. 55 (2016) 5090-5095.

[26] A. Eguia-Barrio, E. Castillo-Matrinez, X. Liu, R. Dronskowski, M. Armand, and T. Rojo, Carbodiimides: new materials applied as anode electrodes for sodium and lithium ion batteries, J. Mater. Chem. A 4 (2016) 1608-1611.

[27] A. Eguia-Barrio, E. Castillo-Martínez, F. Klein, R. Pinedo, L. Lezama, J. Janek, P. Adelhelm, T. Rojo, Electrochemical performance of CuNCN for sodium ion batteries and comparison with ZnNCN and lithium ion batteries, J. Power Sources 367 (2017) 130-137

[28] Q. Liua, Y. Liua, G. Dai, L. Tian, J. Xua, G. Zhao, Na Zhang, Y. Fang, Size-controllable synthesis of hierarchical copper carbodiimide microcrystals and their pronounced photoelectric response undervisible light, Appl. Surf. Sci. A 357 (2015) 745-749.

[29] D. Ressnig, M. Shalom, J. Patscheider, R. More, F. Evangelisti, M. Antonietti and G. R. Patzke, Photochemical and electrocatalytic water oxidation activity of cobalt carbodiimide, J. Mater. Chem. A 3 (2015) 5072-5082.

[30] M. Krings, G. Montana, R. Dronskowski, and C. Wickleder, Alpha-SrNCN:$Eu^{2+}$ - a novel efficient orange-emitting phosphor, Chem. Mater. 23 (2011) 1694-1699.

[31] J. Sindlinger, J. Glaser, H. Bettentrup, T. Justel and H. J. Meyer, Synthesis of $Y_2O_2(CN_2)$ and luminescence properties of $Y_2O_2(CN_2)$:Eu, Z. Anorg. Allg. Chem., 633 (2007) 1686-1690.

[32] J. Glaser, L. Unverfehrt, H. Bettentrup, G. Heymann, H. Huppertz, T. Justel, and H. J. Meyer, Crystal structures, phase-transition, and photoluminescence of rare earth carbodiimides, Inorg. Chem. 47 (2008) 10455-10460.

[33] M. Kubus, C. Castro, D. Enseling, and T. Justel, Room temperature red emitting carbodiimide compound $Ca(CN_2):Mn^{2+}$, Opt. Mater. 59 (2016) 126-129.

[34] Y. Masubuchi, S. Nishitani, S. Miyazaki, H. Hua, J. Ueda, M. Higuchi, and S. Tanabe, Large red-shift of luminescence from $BaCN_2:Eu^{2+}$ red phosphor under high pressure, Appl. Phys. Exp. 13 (2020) 042009/1-3.

[35] P. Kroll, M. Andrade, X. Yan, E. Ionescu, G. Miehe, and R. Riedel, Isotropic negative thermal expansion in β-$Si(NCN)_2$ and its origin, J. Phys. Chem. C 116 (2011) 526-531.

[36] K. Dolabdjian, A. Kobald, C. P. Romao and H. J. Meyer, Synthesis and thermoelastic properties of $Zr(CN_2)_2$ and $Hf(CN_2)_2$, Dalton Trans. 47 (2018) 10249-10255.

[37] M. Kakihana, “Sol-gel” preparation of high temperature superconducting oxides, J. Sol-Gel Sci. Technol. 6 (1996) 7-55.

[38] M. Kakihana, Synthesis of high-performance ceramics based on polymerizable complex method, J. Ceram. Soc. Jpn. 117 (2009) 857-862.

[39] L. Palatinus and G. Chapuis, *SUPERFLIP* – a computer program for the solution of crystal structures by charge flipping in arbitrary dimentions, J. Appl. Crystallogr. 40 (2007)

786-790.

[40] G. M. Sheldrick, Crystal structure refinement with *SHELXL*, Acta Crystallogr. Sect. C 71 (2015) 3-8.

[41]. K. Momma and F. Izumi, VESTA 3 for three-dimensional visualization of crystal, volumetric and morphology data, J. Appl. Crystallogr. 44 (2011) 1272-1276.

[42] R. Oishi-Tomiyasu, M. Yonemura, T. Morishima, A. Hoshikawa, S. Torii, T. Ishigaki and T. Kamiyama, Application of matrix decomposition algorithms for singular matrices to the Pawley method in *Z-Rietveld*, J. Appl. Crystallogr. 45 (2012). 299-308.

[43] F. Izumi and K. Momma, Three-dimensional visualization in powder diffraction, Solid State Phenom. 130 (2007) 15-20.

[44] Y. Hashimoto, M. Takahashi, S. Kikkawa, and F. Kanamaru, Synthesis and crystal structure of a new compound, lanthanum dioxymonocyanamide ($La_2O_2CN_2$) J. Solid State Chem. 114 (1995) 592-594.

[45] W. H. Baur, The rutile type and its derivatives, Crystallogr. Reviews, 13 (2007) 65-113.

[46] K. Fujii, Y. Yoshida, Y. J. Shan, K. Tezuka, Y. Inaguma, and M. Yashima, Cation- and anion-ordered rutile-type derivative $LiTeO_3(OH)$, Chem. Commun. 56 (2020) 10042-10045.

[47] C. Braun, L. Mereacre, W. Hua, T. Sturzer, I. Ponomarev, P. Kroll, A. Slabon, Z. Chen, Y. Damour, X. Rocquefelte, J.-F. Halet, and S. Indris, $SnCN_2$: a carbodiimide with an innovative

approach for energy storage systems and phosphors in modern LED technology ChemElectroChem, 7 (2020) 4550-4561.